DOI: 10.1002/((please add manuscript number))
Article type: Communication

Microfluidic Gel Patterning by use of a Temporary Membrane for Organ-On-Chip Applications

Martijn P. Tibbe, Anne M. Leferink, Albert van den Berg, Jan C.T. Eijkel and Loes I. Segerink*

Ir. M.P. Tibbe, Dr. ir. A.M. Leferink, Prof. dr. ir. A. van den Berg, Prof. dr. J.C.T. Eijkel, Dr. ir. L.I. Segerink
University of Twente, P.O. box 217, 7500 AE, Enschede, the Netherlands
E-mail: l.i.segerink@utwente.nl

Keywords: membranes, organs-on-chips, chitosan, hydrogel, blood-brain barrier

Traditional two-dimensional (2D) and three-dimensional (3D) culture systems allow for analysis of tissue cultures comprising of one or more cell types. In 3D cell culture systems, researchers attempt to mimic the native cellular microenvironment *in vitro* by using engineered scaffolds or hydrogels allowing for the cells to experience specific physicochemical cues. Moreover, cell culture platforms can be designed inside microfluidic chips to allow for controlled fluid flow resulting in a dynamic, more physiological relevant microenvironment [1]. When these microfluidic systems are used to model physiological functions of tissues and organs, they are called organs-on-chips (OOCs) [2]. The field of OOCs is rapidly emerging due to the growing interest in its applications. In general, OOC devices contain one or multiple cell types, and can be used for several purposes such as drug screening [3] or disease modelling [4]. Several organs, such as the lung, the gut and the blood-brain barrier (BBB) have already successfully been developed on chip [5].

Most organs function due to the interaction between two tissue sides, the parenchymal side and the vascular endothelium side. This interface is strengthened by connective tissue that is often referred to as the basal lamina or basement membrane [6]. Recreating this native interface on-chip is challenging, mostly due to the limitations that come with microfluidic chip design. Therefore, porous membranes usually made of polycarbonate (PC) [5c, 5d, 7],

polydimethylsiloxane (PDMS) [5a, 5b, 8] or poly-ethylene terephthalate (PET) [9] are used to mimic the basal lamina function acting as a mechanically stable cell substrate and separating two microchannels from each other. As cells are cultured in these channels, the porous membrane serves as a cell-support and functions as a permanent or temporary interface between parenchymal and endothelial tissues allowing them to create basal lamina like structures. Factors such as the porosity, pore size and membrane thickness determine the amount of signal transportation between cell types over the membrane. Large pores, with a pore size of approximately 20 µm and larger, allow for cells to enter the membrane and reach the other cell layer, depending on the thickness, the pore interconnectivity and pore tortuosity of the membrane. Cells penetrating the membrane will have a negative influence on transmembrane measurements. Smaller pores allow for paracrine signalling through the membrane, but disallow direct cell-cell contact. Additionally, the commercially available polymer membranes do not resemble the physiological basement membrane stiffness and are therefore not suitable for realistic OOC applications. To obtain a more physiological relevant OOC system, the barrier between the parenchymal channel and the endothelial channel should allow for direct cell-cell contact without inducing a negative influence on membrane characterization. The use of a temporary membrane will create the opportunity to remove the membrane to establish a co-culture of multiple cell types without having an artificial/synthetic membrane on-chip. Removing the artificial membrane between two cell types induces the endothelial cells to produce native basal lamina which creates a stable basement membrane between parenchymal and endothelial cells [10].

When we take for example a BBB on a chip, the influence of the brain microenvironment on the permeability of the BBB is so far unclear. There is, however, a strong indication that an increase in endothelial tight junction complexes is induced by direct contact between brain endothelial cells and astrocytes [11]. The presence of a physical membrane separating the endothelial cells from the astrocytes on a microfluidic chip is thought to have an influence on

the intercellular contact of the endothelial cells. Therefore, systems in which astrocytes and endothelial cells are in direct contact with each other are preferred.

A recent study has shown that it is possible to create a membrane on-chip by having an interfacial polymerization reaction at the interface of two liquids. Zhang *et al.* presented a method to create free-standing polymer films by interfacial polymerization [12]. This reaction resulted in two channels, separated by a thin, nanoporous polyamine film. However, removal of this film requires a chemical reaction, unfavorable for the application in an OOC system in which cells are cultured. A reversible membrane fabrication method that will not potentially induce cytotoxicity is therefore required. Chitosan is a biodegradable biomaterial that is suited for membrane production in less harsh non-cytotoxic conditions and is therefore a promising candidate for temporary membranes in OOCs. Chitosan is a polysaccharide derived from the full or partial N-deacetylation of chitin. Chitosan can be protonated after which it becomes soluble in an acidic solution. The opposite reaction, deprotonation of chitosan with a basic buffer, is used by Luo *et al.* to create a membrane on-chip which they used for bacterial cell signaling studies [13]. With this deprotonation method, free-standing, semi-permeable chitosan membranes can be created that have extracellular matrix like properties such as comparable stiffness, high water content and good cell adhesion.

In this research, we propose a method to create chitosan membranes on-chip to be used as temporary barriers in OOC systems and we show that this can be applied to a BBB on-chip. We make use of the solubility of chitosan in acidic conditions to remove the membrane, after fulfilling its primary function as cell substrate, to obtain a membrane-free OOC system. As a starting point, the chip design described by Luo *et al*. was tested, whereby we took the design that included an extra downstream input to balance the pressure at the outlets. We observed, that the downstream flow in this lay-out generally prevented proper membrane attachment at the distal point precluding a stable and reproducible membrane formation [14]. To better guide the growing chitosan membrane to the distal point, we therefore designed and fabricated a new

chip by adding an extra outlet (marked with number 5 in Figure 1A) that serves as a fluidic guide for the membrane compared to the designs of Luo *et al* [13-14] (Figure 1A and Figure 1B). As can be seen in Figure S1, the membrane starts to form 10 seconds after the chitosan arrives at the origin. After 1 minute, the membrane has reached the extra outlet. Chitosan flow is continued for 10 minutes to create a closed membrane from origin to distal point with sufficient thickness to separate the two channels.

As can be seen in Figure 1A and Figure 1C a chitosan solution of 0.5% w v^{-1}, is focused between a neutral carbonate buffer (pH 7.0) and a basic phosphate buffer (pH 9.6). To operate the device, first a stable fluid interface between the phosphate and carbonate buffer is established. Due to the comparable viscosity of the two buffers, both fluid flows are set to 200 µL min^{-1}. As soon as a stable interface is established, the chitosan solution is introduced with a lower flow rate of 20 µL min^{-1}, to compensate for the two times higher viscosity of the solution [15] (Figure 1C). After 10 minutes, a stable membrane is formed from origin to distal point and the fluid flow is turned off. To ensure no further deprotonation, which would result in a thicker membrane, all channels are subsequently perfused with a pH-neutral buffer solution.

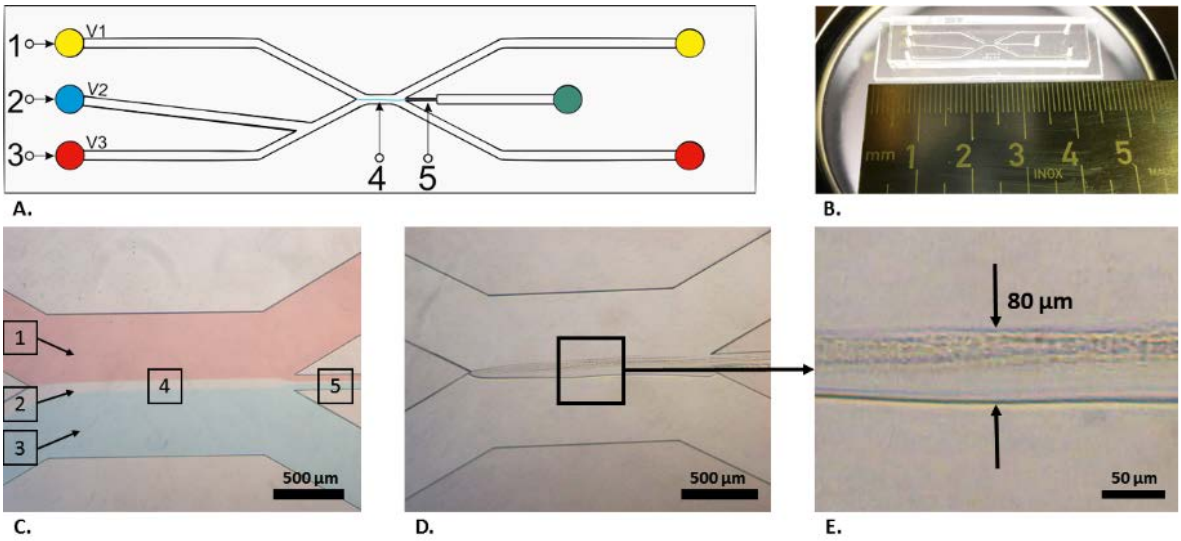

Figure 1. Schematic chip design. (A) A basic buffer (pH 9.6) is inserted via inlet 1 (V1). The chitosan solution is inserted via inlet 2 (V2). The neutral buffer (pH 7.0) is introduced via inlet 3 (V3). This buffer focusses the chitosan to the center of the chip as indicated with number 4 towards the extra outlet indicated with number 5. (B) Image of the PDMS chip. (C) Bright field image of the chip at t=0. The basic buffer V1 is stained red whereas the neutral buffer V3 is stained blue. Chitosan is left unstained. (D) Bright field image of a chitosan membrane after 10 minutes formation. (E) Enlargement of the chitosan membrane from Fig 1D. The thickness of the membrane is approximately 80 µm.

After preparation, it was observed that the membrane had a sharp delimitation at the acidic side and a diffuse border at the basic buffer side (Figure 1E). During the formation of the membrane, the growth was at the acidic side of the membrane. Since the hydroxyl ions diffuse much faster than the larger chitosan molecules, we assume that the membrane growth is due to the diffusion of hydroxyl ions through the chitosan membrane. We assessed the thickness by measuring the thickness in bright field microscopy images of the formed membrane over time (Figure 2). The growth of the membrane slows down over time as was also observed by Luo *et al* [13]. The diffusional flux of hydroxyl ions which determines the actual thickness is dependent on the pH gradient and membrane thickness. The average diffusion distance (x) of ions can be described by the following equation: $x = \sqrt{2Dt}$, with t the time and D the diffusion constant. If we fit this equation to our measurement data, we obtain a good fit (R^2=0.91) for a diffusion constant through the membrane of $17.1 \cdot 10^{-11}$ m^2 s^{-1}, which is about 100 times lower than the diffusion constant in water [16]. Additionally, we notice that, on average, the thickness of the membrane

reaches a plateau, leading to a constant thickness of 128 µm after 7 minutes, indicating that the hydroxyl ions do not diffuse further through the membrane (Figure 2).

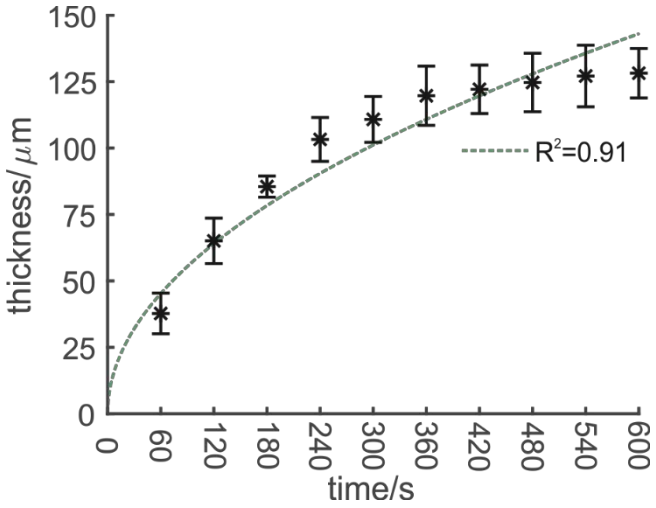

Figure 2. Increase in chitosan membrane thickness over time. Asterisks show the actual measured thickness of the membrane at time intervals of 60 seconds and the error bars indicate the standard deviation. The green dotted line shows the fit of the formula $x = \sqrt{2Dt}$ with a diffusion constant of $17.1 \cdot 10^{-11}$ m^2 s^{-1}.

It is important to note that the thickness of the membrane can vary per experiment whilst the formation is influenced by factors as the fluid viscosities which are dependent on room temperature. Also, small impurities or obstructions in the microfluidic channels can cause the membrane to grow thicker or thinner compared to the average shown in figure 2. To assess the influence of the concentration of chitosan in the solution on the thickness of the membrane, two solutions with concentrations of 0.25% and 1.0% w v^{-1} were also applied to produce membranes. However, no major differences were observed in the formation and final thicknesses of these membranes (Table S1).

The membrane formation is a reversible process. A membrane-free system is created by dissolving the chitosan membrane via protonation. This is induced by flushing an acetic acid solution (pH 5.0) through one channel. With a flow speed of 75 µL min^{-1}, it takes the acid 60 seconds to fully dissolve a membrane with a length of 1500 µm (Movie S1). Consequently, 2000 µm long membranes with the same thickness, will need 25% more acid and time to

dissolve. To validate full membrane removal, chitosan is fluorescently labeled with NHS-fluorescein prior to membrane formation (Movie S2).

To explore the applicability of this removable membrane in an OOC device and more specifically in a BBB on-chip, cells are seeded and cultured into the chip. Human astrocytes (retrieved from the cerebral cortex) are chosen as the parenchymal cell type to be cultured in this BBB on-chip system. Once a stable chitosan membrane is formed in the chip, astrocytes incorporated into the natural extracellular matrix based hydrogel Matrigel are seeded through inlet 2 and 3 (Figure 1A). Matrigel is a temperature responsive hydrogel that forms a solid gel after a few hours at 37°C. The chitosan membrane provides a mechanically strong barrier preventing the cell-laden Matrigel from running into the opposite channel as is shown in Figure 3A. The opposing channel is continuously perfused with astrocyte medium during seeding to prevent the membrane from collapsing due to pressure differences. The morphology of the astrocytes seeded in the Matrigel is similar to the morphology of the same type of astrocytes cultured in a standard tissue culture flask (Figure S2). Astrocytes are stained fluorescently with a cell tracker (Figure 3A) to see whether they would pass the membrane. As can be seen from Figure 3A and Figure 3D, astrocytes are only present in the channel in which they were seeded indicating the disability of the cells to pass the chitosan membrane. After 18 hours the astrocytes become attached to the hydrogel and start to adapt their elongated morphology (Figure 3D) which they also show in their physiological microenvironment [17]. A next step is to remove the chitosan membrane. Due to the high collagen content in Matrigel, it will be dissolved when it encounters acetic acid upon membrane removal. Therefore, in contrast to membrane-removal in the gel-free system as mentioned above, the exact amount and residence time of acetic acid required to dissolve only the chitosan and not the Matrigel was calculated and found to be 75 µL and 60 seconds, respectively (Figure 3B and Figure 3E). Phosphate buffer saline (PBS) is perfused continuously through the empty channel, prior to, and after removal of the membrane with acetic acid to remove excess acid. Comparing the morphology of the astrocytes in Figure

3D and Figure 3E, it can be concluded that membrane removal does not have an influence on cell morphology in the gel. To control cell viability after membrane removal, a live/dead cell viability assay was conducted on the astrocytes at the interface (Figure S3 and Figure S4).

After membrane removal, brain microvascular endothelial cells (BMVECs, hCMEC/D3) are seeded into the empty channel (inlet 1 in Figure 1). These endothelial cells grow on the surface of the Matrigel forming an interface with the astrocytes (Figure 3C and Figure 3F in green), without having a membrane between the cell types. To show cell-cell contact at the interface, high magnification images were taken at various focal planes, combined as a z-project image in Fiji [18] and stitched in a full channel-width figure in Photoshop (Figure S5).

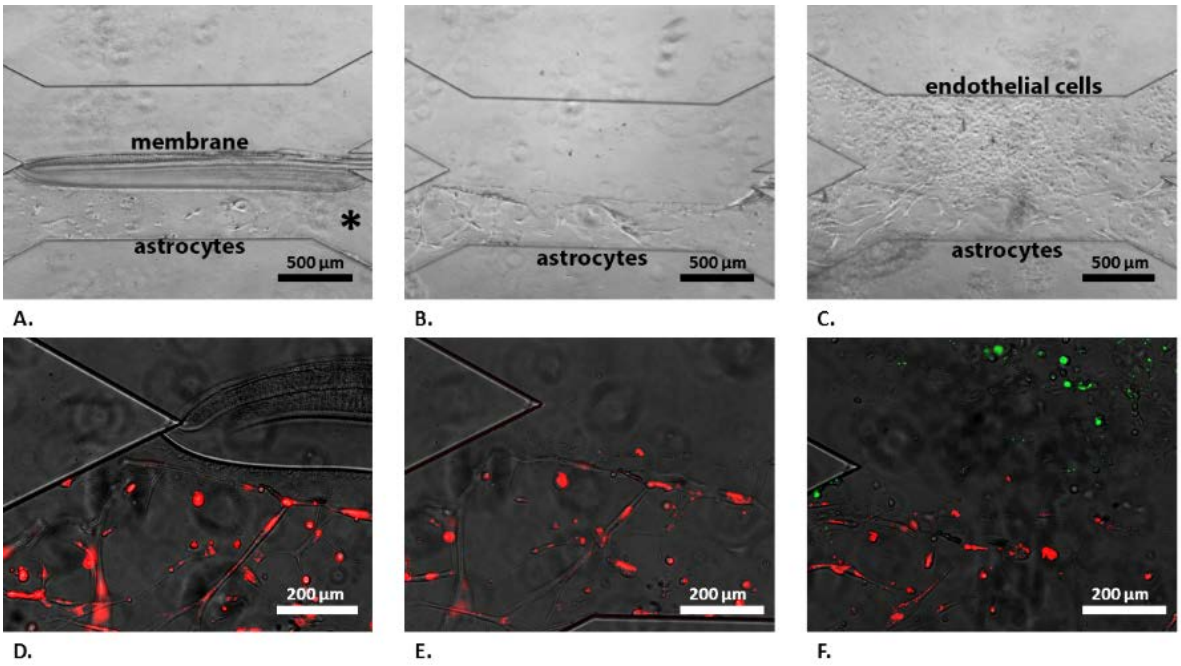

Figure 3. After membrane formation, the system is perfused with astrocyte medium prior to astrocyte seeding to remove excess chitosan and basic buffer. Astrocytes in Matrigel are seeded from the outlet marked with an asterix (*). Astrocytes are homogeneously distributed through the Matrigel (A, D). 18 Hours after seeding the astrocytes, an acetic acid solution with pH 5.0 is flushed through the empty channel resulting in total removal of the chitosan membrane. The morphology of the astrocytes is not influenced by the removal of the membrane (B, E). Prior to seeding endothelial cells in the empty channel, the channel is coated with a fibronectin solution. Brain-endothelial cells (hCMEC/D3) are now seeded into the empty channel. 24 Hours after hCMEC/D3 seeding, the cells reach almost 100 percent confluence in the channel. However, when there is no membrane present, it is possible for the astrocytes to migrate out of the gel into the empty channel. Therefore, endothelial cell seeding should be conducted directly after membrane removal. HCMEC/D3 cells were stained green with a DiO cell-tracker (C, F). Astrocytes were stained red with a DiI cell-tracker to see the cell distribution inside the channel.

As a proof of concept, we applied a slight adjustment in the chip design and demonstrated that two membranes can be made in a single chip creating three separated channels (Figure S6). Chitosan is introduced through a small, 100 µm wide, middle inlet where it comes in contact on two sides with the basic buffer and gets deprotonated. By increasing the flow speed of chitosan to 30 µl min^{-1} and decreasing the flow speed of the basic buffer to 100 µl min^{-1} an open channel in between the two membranes is formed. Increasing the basic buffer flow rate will result in merging of the membranes and thus a closed center channel. Decreasing the basic buffer flow rate will result in a wider middle channel, up to 100 µm.

In this study, a method to obtain a mechanically stable membrane of chitosan in a microfluidic channel was presented. Although this method translates to any other crosslinkable material that can have their polymerization or gelation reaction on a liquid-liquid interface [12, 19], a reversible and biocompatible reaction, such as the reaction shown in this study, can only be achieved when the membrane material is not covalently cross-linked. A candidate material for a method similar as the one presented here is the polysaccharide alginate that is ionically cross-linked by divalent cations to form a hydrogel. However, despite the biocompatibility of alginate, it lacks the ability for cells to bind to the extremely hydrophilic polymer chains. Yet, the cell binding capability of alginate can be improved by de addition of arginylglycylaspartic acid (RGD) groups [20].

Summarizing, by using a removable chitosan membrane, we can successfully pattern cell-laden hydrogels inside a microfluidic chip without the use of structural additions such as columns in the channel to hold the gel in place[21]. The latter is the traditional approach limiting the interfacial contact area which resembles the cell-barrier. It was possible to create a co-culture of human astrocytes and brain endothelial cells inside our microfluidic system where we observed direct cell-cell contact between the two cell types (Figure S5). This technique offers the user a tool to temporarily create barriers on chip to be used for hydrogel or cell patterning. We also showed that by adding an extra inlet to the chip, it was possible to create two membranes simultaneously.

Experimental Section

Device Design and Fabrication: SU-8 patterned, 4" silicon wafers that will serve as mold for multiple polydimethylsiloxane (PDMS) chips were made by photo-lithography in a cleanroom environment. PDMS base agent was mixed with PDMS curing agent in a 10:1 wt. ratio (Sylgard 184 Silicone elastomer kit, Dow Corning, Midland, MI, USA). To remove entrapped air bubbles, the PDMS was degassed prior to pouring it onto the SU-8 patterned wafer using a desiccator. After pouring the PDMS over the SU-8 patterned wafer, the PDMS was cured at 60°C for 4 hours. The cured PDMS slap was demolded from the SU-8 patterned wafer and cut into individual chips. Fluidic inlets, with a diameter of 1 mm, were punched into the PDMS chips. Prior to bonding the PDMS chips, the chips and glass microscopy slides are exposed (bond-side up) to an oxygen plasma for 45 seconds. To ensure the bond, the chips are incubated at 60°C for at least 6 hours.

Chitosan preparation: A chitosan solution was prepared by adding chitosan flakes (medium molecular weight, average weight 300 000 g mol^{-1}, Sigma-Aldrich Chemie GmbH, Steinheim, Germany) to deionized-water. The solution is brought to a pH of 3 by adding 99% HCl (Sigma-Aldrich Chemie GmbH, Steinheim, Germany) dropwise. After stirring the solution overnight NaOH can be added to increase the pH to 5. DI-water is added to bring the solution to 0.5% w v^{-1} if necessary. The final chitosan solution is filtered using a 0.2 µm syringe filter (Millex, Merck Millipore, Tullagreen, Cork, Ireland).

An NHS-fluorescein solution is made by adding 2.5 mg NHS-fluorescein (Thermo Scientific, Rockford, IL, USA) to 200 µL dimethylformamide (DMF, Sigma-Aldrich Chemie GmbH, Steinheim, Germany) and 800 µL 99% ethanol. To label chitosan fluorescently, 1 µL of NHS-fluorescein solution is added to 2.5 mL of chitosan 0.5% w v^{-1}.

Cell seeding and staining: For recreation of the parenchymal tissue in this chip, human astrocytes from the cerebral cortex (hAstro, passage 6-10, ScienCell Research Laboratories, Corte Del Cedro Carlsbad, CA, USA) are used. Astrocytes are cultured in poly-l-lysine (PLL, 2 µg mL in PBS 1h at 37°C)(Sigma-Aldrich Chemie GmbH, Steinheim, Germany) coated T75 tissue culture flasks with astrocyte medium (AM, 500 mL of basal medium, 10 mL of fetal bovine serum (FBS), 5 mL of astrocyte growth supplement (AGS) and 5 mL of penicillin/streptomycin solution (P/S) (ScienCell Research Laboratories, Corte Del Cedro Carlsbad, CA, USA)). The astrocytes are incubated at 37°C in a humidified environment with 5% CO_2. Medium was refreshed every three days. The cell line used to create the vascular side in the described OOC system are human cerebral microvascular endothelial cells (hCMEC/D3 cell line, passage 28-34, kindly provided by Dr. P.-O. Couraud, INSERM, Paris, France). HCMEC/D3 cells are cultured in collagen coated T75 flasks (CELLCOAT, Greiner Bio One, Kremsmünster, Austria). Cells are incubated in humidified air at 37°C with 5% CO_2. Medium was refreshed every two days.

Astrocytes were mixed at room temperature in a 1:2 ratio with Matrigel (ECM-matrix, Corning, Tewksbury, MA, USA) with an end concentration of astrocytes of 3×10^6 cells mL^{-1} in the gel. After injecting 30 µL of Matrigel solution into the chip, the chip is incubated at 37°C, humidified air with 5% CO_2, for 24 hours to let the solution form a gel. After 24 hours, the membrane is removed by flushing an acetic acid solution (pH5) through the opposing channel. For a membrane of 75 µm high and 1500 µm long, 75 µL acetic acid is used. After membrane removal, hCMEC/D3 cells in 30 µL EGM-2 are seeded 3×10^6 cells mL^{-1} in the opposing channel. Hydrostatic pressure was applied to the cells by placing pipette tips with unequal medium amounts on the inlets and outlets (150 µL and 100 µL respectively).

To stain the hCMEC/D3 cells and astrocytes, detached cells are suspended at a density of 1×10^6 cells mL^{-1} in PBS. Per milliliter of cell suspension, 5 µL cell tracker (DiI or DiO, Vybrant™, Invitrogen™, Thermo Fisher Scientific, Waltham, MA, USA) is added. The stained cells are

incubated for 30 minutes at 37 °C. After 30 minutes, the cell suspension is centrifuged for 5 minutes at 1500 rpm. The supernatant was removed and cells were resuspended in warm (37 °C), cell specific medium to obtain the correct concentration. The cells are washed 2 times with medium. Cells were imaged by phase contrast and fluorescently by use of an EVOS XL microscope (EVOS®, Hatfield, PA, USA).

Seeded cells are stained with ActinGreen™ 488 and NucBlue© (both Invitrogen Molecular Probes™, Thermo Fisher Scientific, Waltham, MA, USA) after treatment with 1% Triton-x (Sigma-Aldrich Chemie GmbH, Steinheim, Germany). One drop of each staining solution is added to 1 mL of cell media that is perfused through the chip.

Acknowledgements

This work was supported by the ERC who provided us with the ERC advanced grant VESCEL. We thank Paul ter Braak for his experimental assistance. We would also like to thank prof. dr. Rob Lammertink, dr. Andries van der Meer and ir. Marinke van der Helm for the useful discussions.

Received: ((will be filled in by the editorial staff))
Revised: ((will be filled in by the editorial staff))
Published online: ((will be filled in by the editorial staff))

References

[1] D. Huh, G. A. Hamilton, D. E. Ingber, **2011,** *21* (12), 745-754.
[2] a) S. N. Bhatia, D. E. Ingber, **2014,** *32* (8), 760-772; b) F. Zheng, F. Fu, Y. Cheng, C. Wang, Y. Zhao, Z. Gu, **2016,** *12* (17), 2253-2282.
[3] a) S. L. Faley, M. Copland, D. Wlodkowic, W. Kolch, K. T. Seale, J. P. Wikswo, J. M. Cooper, **2009,** *9* (18), 2659-2664; b) Z. Xu, Y. Gao, Y. Hao, E. Li, Y. Wang, J. Zhang, W. Wang, Z. Gao, Q. Wang, **2013,** *34* (16), 4109-4117.
[4] a) A. Gunther, S. Yasotharan, A. Vagaon, C. Lochovsky, S. Pinto, J. Yang, C. Lau, J. Voigtlaender-Bolz, S.-S. Bolz, **2010,** *10* (18), 2341-2349; b) E. Westein, A. D. van der Meer, M. J. E. Kuijpers, J.-P. Frimat, A. van den Berg, J. W. M. Heemskerk, **2013,** *110* (4), 1357-1362.
[5] a) D. Huh, B. D. Matthews, A. Mammoto, M. Montoya-Zavala, H. Y. Hsin, D. E. Ingber, **2010,** *328* (5986), 1662-1668; b) H. J. Kim, D. Huh, G. Hamilton, D. E. Ingber, **2012,** *12* (12), 2165-2174; c) R. Booth, H. Kim, **2012,** *12* (10), 1784-1792; d) M. W. van der Helm, M. Odijk, J.-P. Frimat, A. D. van der Meer, J. C. T. Eijkel, A. van den Berg, L. I. Segerink, **2016,** *85*, 924-929; e) M. W. van der Helm, A. D. van der Meer, J. C. T. Eijkel, A. van den Berg, L. I. Segerink, **2016,** *4* (1), e1142493.
[6] K. M. Baeten, K. Akassoglou, **2011,** *71* (11), 1018-1039.

[7] a) L. M. Griep, F. Wolbers, B. Wagenaar, P. M. Braak, B. B. Weksler, I. A. Romero, P. O. Couraud, I. Vermes, A. D. Meer, A. Berg, **2012,** *15* (1), 145-150; b) A. K. H. Achyuta, A. J. Conway, R. B. Crouse, E. C. Bannister, R. N. Lee, C. P. Katnik, A. A. Behensky, J. Cuevas, S. S. Sundaram, **2013,** *13* (4), 542-553; c) J. A. Brown, V. Pensabene, D. A. Markov, V. Allwardt, M. D. Neely, M. Shi, C. M. Britt, O. S. Hoilett, Q. Yang, B. M. Brewer, P. C. Samson, L. J. McCawley, J. M. May, D. J. Webb, D. Li, A. B. Bowman, R. S. Reiserer, J. P. Wikswo, **2015,** *9* (5), 054124.
[8] D. Huh, Y.-s. Torisawa, G. A. Hamilton, H. J. Kim, D. E. Ingber, **2012,** *12* (12), 2156-2164.
[9] F. R. Walter, S. Valkai, A. Kincses, A. Petnehazi, T. Czeller, S. Veszelka, P. Ormos, M. A. Deli, A. Der, **2016,** *222*, 1209-1219.
[10] A. Herland, A. D. van der Meer, E. A. FitzGerald, T.-E. Park, J. J. F. Sleeboom, D. E. Ingber, **2016,** *11* (3), e0150360.
[11] a) J. A. Holash, D. M. Noden, P. A. Stewart, **1993,** *197* (1), 14-25; b) N. J. Abbott, L. Rönnbäck, E. Hansson, **2006,** *7* (1), 41-53; c) N. J. Abbott, A. A. K. Patabendige, D. E. M. Dolman, S. R. Yusof, D. J. Begley, **2010,** *37* (1), 13-25; d) F. L. Cardoso, D. Brites, M. A. Brito, **2010,** *64* (2), 328-363.
[12] Y. Zhang, N. E. Benes, R. G. H. Lammertink, **2015,** *15* (2), 575-580.
[13] X. Luo, D. L. Berlin, J. Betz, G. F. Payne, W. E. Bentley, G. W. Rubloff, **2010,** *10* (1), 59-65.
[14] X. Luo, H. C. Wu, C. Y. Tsao, Y. Cheng, J. Betz, G. F. Payne, G. W. Rubloff, W. E. Bentley, **2012,** *33* (20), 5136-5143.
[15] a) W. M. Haynes, Concentrative Properties of Aqueous Solutions: Density, Refractive Index, Freezing Point Depression, and Viscosity. In *CRC Handbook of Chemistry and Physics*, Haynes, W. M., Ed. CRC Press: 2013-2014; b) A. Martínez, E. Chornet, D. Rodrigue, **2004,** *35* (1), 53-74.
[16] S. H. Lee, J. C. Rasaiah, **2011,** *135* (12), 124505.
[17] a) M. A. Olude, O. A. Mustapha, O. A. Aderounmu, J. O. Olopade, A. O. Ihunwo, **2015,** *9*, 67; b) M. V. Sofroniew, H. V. Vinters, **2010,** *119* (1), 7-35.
[18] J. Schindelin, I. Arganda-Carreras, E. Frise, V. Kaynig, M. Longair, T. Pietzsch, S. Preibisch, C. Rueden, S. Saalfeld, B. Schmid, J.-Y. Tinevez, D. J. White, V. Hartenstein, K. Eliceiri, P. Tomancak, A. Cardona, **2012,** *9* (7), 10.1038/nmeth.2019.
[19] C. Hong, K. Rachel, R. Zimei, S. Andrei, V. Pankaj, **2010,** *2* (3), 035002.
[20] a) K. Y. Lee, D. J. Mooney, **2001,** *101* (7), 1869-1880; b) K. Y. Lee, D. J. Mooney, **2012,** *37* (1), 106-126; c) J. M. Silva, A. R. C. Duarte, S. G. Caridade, C. Picart, R. L. Reis, J. F. Mano, **2014,** *15* (10), 3817-3826.
[21] M. Kang, W. Park, S. Na, S.-M. Paik, H. Lee, J. W. Park, H.-Y. Kim, N. L. Jeon, **2015,** *11* (23), 2789-2797.